Pamukkale Üniversitesi Mühendislik Bilimleri Dergisi
Pamukkale University Journal of Engineering Sciences

Investigation of the microstructure and tensile properties of dual-phase steels of different strength levels joined by resistance spot welding

Nokta direnç kaynağı ile birleştirilen farklı dayanım seviyelerine sahip çift fazlı çeliklerin mikroyapı ve çekme özelliklerinin incelenmesi

Emre KATILMIŞ[1], Muhammed ELİTAŞ[2]*

[1]Karabuk University, Graduate Education Institute, Department of Manufacturing Engineering, Karabük, Turkey.
emrekatilmis@hotmail.com
[2]Bilecik Şeyh Edebali University, Faculty Of Engineering, Department Of Mechanical Engineering, Bilecik, Turkey.
muhammed.elitas@bilecik.edu.tr

Received/Geliş Tarihi: 22.06.2024 Revision/Düzeltme Tarihi: 23.09.2024 doi: 10.5505/pajes.2024.24992
Accepted/Kabul Tarihi: 23.10.2024 Research Article/Araştırma Makalesi

Abstract

In this study, DP600/DP1000 and DP600/DP1200 resistance spot welding processes were performed. Welding applications were carried out at 7 kA constant welding current and 5 different electrode pressures (2, 3, 4, 5 and 6 Bar). The study focused on microstructural analysis, microhardness and tensile-shear testing. It was found that the welds consisted of 3 distinct regions. The microstructure differed between the regions. The volume fraction of martensite increased in the weld metal. As the electrode pressure decreased, the tensile-shear force increased for both joint types. The failures occurred on the DP600 side. The pull-out type failure occurred in all joints. Hardness values increased from base metal to weld metal in all parameters.

Keywords: Resistance spot welding, Microstructure, Tensile-shear force, Pull-out type failure, Microhardness

Öz

Bu çalışmada, DP600/DP1000 ve DP600/DP1200 nokta direnç kaynak işlemleri gerçekleştirilmiştir. Kaynak uygulamaları 7 kA sabit kaynak akımı ve 5 farklı elektrot basıncında (2, 3, 4, 5 ve 6 Bar) gerçekleştirilmiştir. Çalışma mikroyapısal analiz, mikrosertlik ve çekme-makaslama testlerine odaklanmıştır. Kaynakların 3 farklı bölgeden oluştuğu tespit edilmiştir. Mikroyapı, bölgeler arasında farklılık göstermiştir. Kaynak metalinde martenzit hacim oranı artmıştır. Elektrot basıncı azaldıkça çekme-makaslama kuvveti her iki bağlantı tipi için de artmıştır. Kırılmalar, DP600 tarafında meydana gelmiştir. Düğme tipi kırılma tüm bağlantılarda meydana gelmiştir. Sertlik değerleri tüm parametrelerde esas metalden kaynak metaline doğru artmıştır.

Anahtar kelimeler: Nokta direnç kaynağı, Mikroyapı, Çekme-makaslama kuvveti, Düğme tipi kırılma, Mikrosertlik

1 Introduction

Advanced High Strength Steels (AHSS) are preferred in the automotive industry due to their benefits such as weight reduction, and cost savings [1], [2]. Not only do AHSS allow vehicles to be made lighter than other steels, but they also have tensile strengths in excess of 600 MPa. The tensile strength of high strength steels (HSS) varies between 400-440 MPa. AHSS have a higher yield strength and a high strain energy absorption capacity. AHSS therefore reduce the weight of the vehicle without reducing its strength and can absorb similar or higher levels of impact energy [3].

Dual-phase (DP) steels, a type of AHSS, are preferred in the automotive industry due to their combination of high strength and ductility and good formability. DP steels are produced from high-strength, low-alloy steels by a critical anneal-quench heat treatment. Although there are microstructures such as small amounts of retained austenite, pearlite, and bainite, the DP expression is due to the ferrite and martensite phases that form the microstructure [4].

The toughness of DP steels is related to the volume ratio of the martensite phase and the ductility is related to the volume ratio of the ferrite phase. The ability to obtain the desired mechanical properties by adjusting the phase volume ratios according to the Lever rule is an important advantage of DP steels. In addition to the chemical composition, it is also very important to determine the production conditions and heat treatment steps in order to achieve ideal DP steel properties [4].

DP steels can be joined by various methods. However, Resistance Spot Welding (RSW) is the preferred method for joining body panels [3], [5]. RSW is preferred because it is economical and does not consume filler material when joining steel sheets [6], [7]. Compared to other welding methods, RSW is most suitable for automation and sustainable engineering [8]. RSW is widely used in the automotive industry [9], [10], [11]. 3000-6000 spots are needed to complete the car bodies [6],[12],[13]. Tensile shear testing (TST) is generally the preferred mechanical test for evaluating the strength of joints [14], [15]. In RSW, the microstructure changes with the high heat input and subsequent rapid cooling. Variations in microstructure are an important factor affecting tensile shear strength (TSS). It is therefore very important to understand and characterize the RSW in order to use DP steels successfully. As mentioned above, the structural performance of the vehicles depends on the structural adequacy of the joints [16]. The studies carried out to investigate the RSW of DP steels are summarized as follows:

Aydin [17] investigated the microstructure and the mechanical properties of dissimilar joints between DP600 and DP1000 steel sheets using different welding currents (WC). He reported

*Corresponding author/Yazışılan Yazar

that the WC significantly affected the microstructure-mechanical properties of the joints, and all the joints exhibited the pull-out failure (PF) mode under TST. Aydin et al.[18] carried out the characterization of the weld zone of automotive sheets of different thicknesses (DP600 and DP800) joined by RSW. They found that the TSS and cross-tensile strength increased in parallel with the increase in WC. Zhang et al. [19] carried out RSW processes to investigate the changes in the mechanical properties of DP780/DP600 materials. It was found that two different failure modes were observed during TST, namely interface (IF) and PF, and the weld metal (WM) size played a dominant role in the failure modes in the joints. Khan et al. [20] performed RSW joints on different material combinations of HSLA350/DP600. They found that the performance of dissimilar combinations was different from that of similar combinations. Yuan et al. [12] performed RSW joints of DP600/DC54D. It was found that as the WC, welding time (WT) and electrode pressure (EP) increased, the TSS value first increased and then decreased. The maximum value (6.59 kN) was obtained at 9 kA-14 cycle–2.6 kN welding parameters. The IF mode was observed due to the small weld nugget (WN) diameter. It was found that PF occurred along the DC54D steel where plastic deformation occurred due to abnormal grain growth in the heat affected zone (HAZ)/base metal (BM) interface region. The DP600/A5052/DP600 RSW combination was realized by Li et al. [21]. The maximum value (10.796 kN) was obtained in 14 cycles of WT. They found that failures occurred at the DP600/A5052 interfaces in the TST due to the Fe_2Al_5 and acicular Fe_4Al_{13} brittle phases.

A review of the literature shows that there are limited studies on RSW joints of different materials. In addition, while there are studies on the effect of WT, and WC parameters on the microstructure and tensile properties of RSW joints, it is observed that EP is addressed in a limited number of studies. Therefore, this study focuses on the effect of EP. It is important to subject different materials to the RSW process in order to combine their superior properties, particularly in terms of strength, and ductility. In the automotive industry, different materials are combined. Therefore, the current study aims to contribute to the industry. In addition, no studies on DP600/DP1000 and DP600/DP1200 RSW combinations were found in the literature. Therefore, it is expected to fill the gap in the literature on this subject.

2 Experimental studies

2.1 Material

The DP600, DP1000 and DP1200 steels were supplied in 500 mm × 500 mm dimensions. The sheet thickness of the DP600 and DP1200 steels is 1 mm, while the thickness of the DP1000 steel is 1.2 mm. For the RSW process, the steel sheets were cut to 100 mm × 30 mm using the Guillotine Shear. The chemical compositions of the steels were determined by spectral analysis (Table 1).

2.2 RSW process

DP600/DP1000 and DP600/DP1200 joints were obtained using 8 mm tip diameter electrodes at a constant WC of 7 kA. To evaluate the effect of EP, experiments were carried out at 5 different EPs. For microstructural analysis and TST, 4 specimens were prepared at all EPs. RSW processes were carried out using a Baykal Brand SPP60 type RSW machine. In addition, wooden fixtures were used to keep the specimens stable during the RSW process (Figure 1). The different DP600/DP1000 and DP600/DP1200 joints obtained after RSW are shown in Figure 2.

Figure 1. Experimental set-up a) RSW machine b) Electrodes c) Wooden fixture [6].

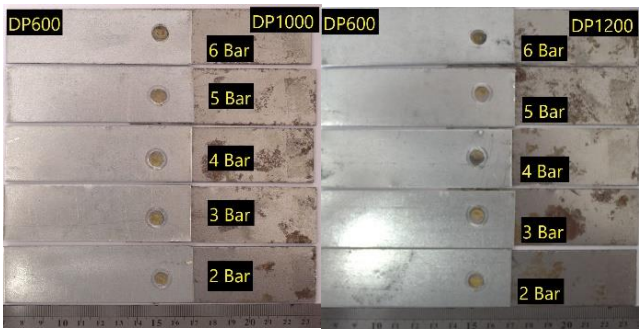

Figure 2. RSW joints.

Table 1. Chemical composition of DP steels (wt%).

Steel	C	Mn	Si	Cr	Ni	Al	Fe
DP600	0.077	1.86	0.253	0.177	0.012	0.127	Balance
DP1000	0.136	1.57	0.203	0.022	0.039	0.044	Balance
DP1200	0.078	1.67	0.190	0.026	0.040	0.044	Balance

2.3 Metallography

In order to examine the microstructure of the DP600/DP1000 and DP600/DP1200 RSW joints, specimens were cut from the centre of the WN using a precision cutting device. Initial grinding was carried out using 120, 220, 360, 600, 800, 1000, 1200, 1500 and 2000 mesh sandpaper. Polishing operations were carried out by using 3 micron and 1 micron diamond solutions. The polished specimens were etched progressively for 2 seconds in 2% Nital (2% Nitric acid + 98% Methanol) solution. The BM, HAZ and WM microstructures were analyzed by Optical Microscopy.

2.4 WN diameter measurement

WN diameter measurements of samples obtained at different EPs were performed using a digital caliper. A schematic representation of the WN diameter is shown in Figure 3.

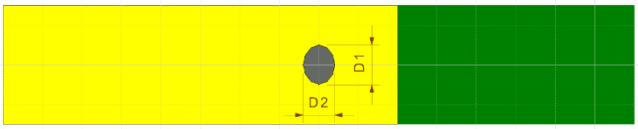

Figure 3. Schematic illustration of WN diameter.

The average WN diameter (d_a) for different EPs was calculated using Equation 1 [6]. The effect of WN diameter on tensile shear force (TSF) values was investigated.

$$d_a = \frac{d_1 + d_2}{2} \quad (1)$$

2.5 TST and failure surface inspection

TSTs were performed at a crosshead speed of 2 mm/min. Tests were performed on 3 specimens for each parameter. TST was performed on a Shimadzu AG-IC 100kN tensile compression testing machine. Different failure modes resulting from TST were captured as macro images using a camera. In addition, detailed microstructural images of the failure surfaces were examined using a ZEISS brand Supra 40 VP model scanning electron microscope (SEM).

2.6 Microhardness test

Microhardness tests were carried out using a Vickers micro hardness tester (Shimadzu) by applying a load of HV 0.5 for 10 s in parallel to the BM, HAZ, and WM axes.

3 Experimental results

3.1 Microstructure

Figure 4 shows an example of the macrostructure weld profile of a DP600/DP1200 RSW sample welded at 7 kA-5 bar. BM, HAZ, and WM optical microscope images of the DP600/DP1000 and DP600/DP1200 joints obtained by the RSW method at 7 kA and 5 bar are shown in Figure 5 and Figure 6, respectively. In addition, WM SEM images of the DP600/DP1000 and DP600/DP1200 joints obtained using the same parameters are shown in Figure 7. Figure 7 shows that the structure consists mainly of the martensite phase.

In the RSW process, as the specimens are subjected to high temperatures and then rapidly cooled, microstructural changes occur. Three different microstructural regions (WM, HAZ, and BM) are observed in RSW joints [19], [21], [22]. When Figure 5 and Figure 6 are evaluated together, the BM microstructure of DP steels consists mainly of ferrite phase and contains small amounts of martensite particles. Similarly, it has been reported that the microstructure of BM is ferrite with a small amount of martensite distributed along the ferrite grain boundary[12], [21]. There is a reduction in the ferrite phase in WM compared to BM. This is because there is an increase in the amount of ferrite dissolved in the austenite phase. A transformation from austenite phase to martensite phase occurs due to rapid cooling [22], [23]. Thus, the martensite volume fraction increased from BM to WM in all EPs. It has been reported that the martensite volume fraction increases in the order of BM, HAZ, and WM[19]. Khan et al. [20] found that the WM of the dissimilar weld (DP600/HSLA350) was predominantly martensitic with some bainite. Li et al. [21] reported that the microstructure of the WM was lath martensite for the DP600 side. In addition, Yuan et al. [12] expressed that the microstructure in the WM was full lath martensite due to the high cooling rate.

3.2 WN diameter

When reviewing the studies on joining DP steels using the RSW method, it was found that there is a direct relationship between the WN diameter and the TSS [6], [24]. According to Dancette et al.[25], a large WN diameter indicates a high loading capacity.

In general, IF occurs because increasing EP causes a decrease in WN diameter. Since static electrical resistance is essentially overcome by EP, EP is an important factor controlling WN formation [26].

The increase in EP reduces the electrical resistance and therefore the heat generated at the sheet/sheet contact surface. As a result, the heat input is lower, resulting in a smaller WN diameter [27]. However, Yuan et al. [12] found that the EP was beneficial for increasing the WN.

WN diameter measurements were carried out on 3 specimens for each parameter. It is observed that the WN diameter values of the DP600/DP1000 and DP600/DP1200 joints obtained at different EPs decrease with increasing EP (Figure 8). Therefore, the results obtained are compatible with the literature.

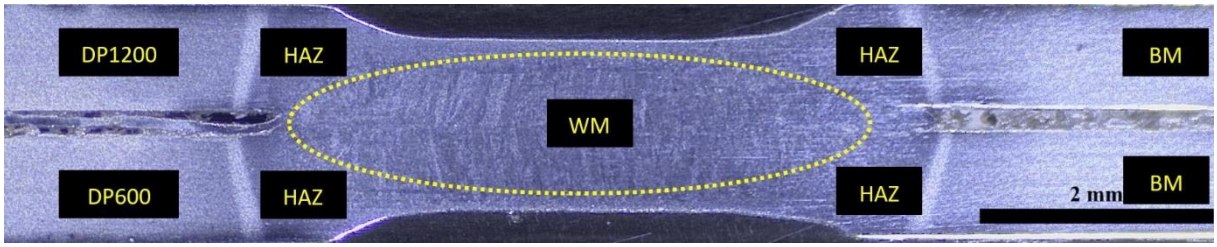

Figure 4. Macrostructure of the DP600/DP1200 RSW sample welded at 7 kA-5 bar.

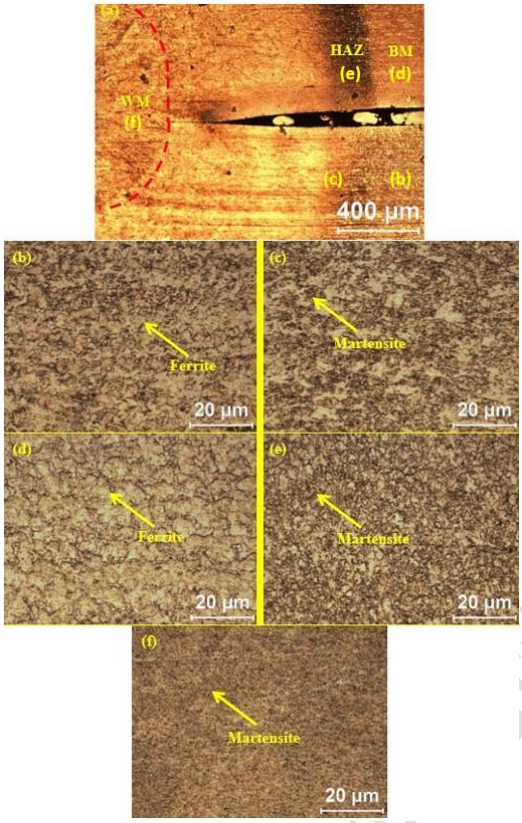

Figure 5. Optical microscope images of RSW DP600/DP1000 joints a) Profile image b) DP600 BM c) DP600 HAZ d) DP1000 BM e) DP1000 HAZ f) WM.

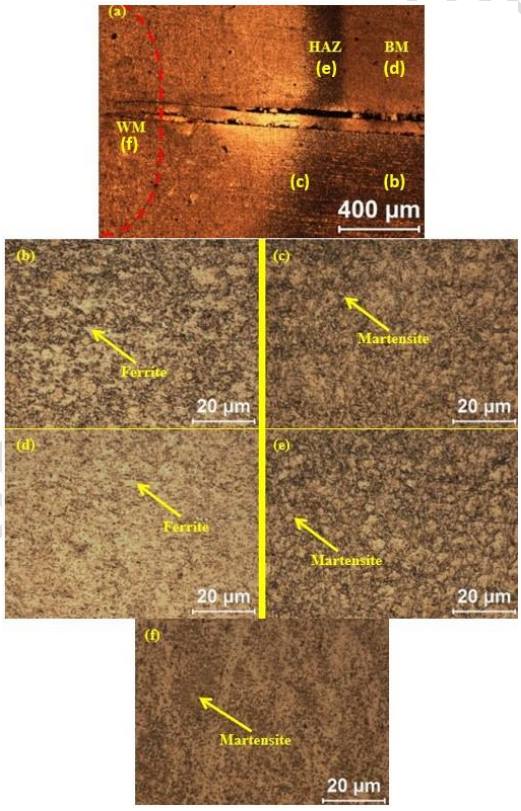

Figure 6. Optical microscope images of RSW DP600/DP1200 joints a) Profile image b) DP600 BM c) DP600 HAZ d) DP1200 BM e) DP1200 HAZ f) WM.

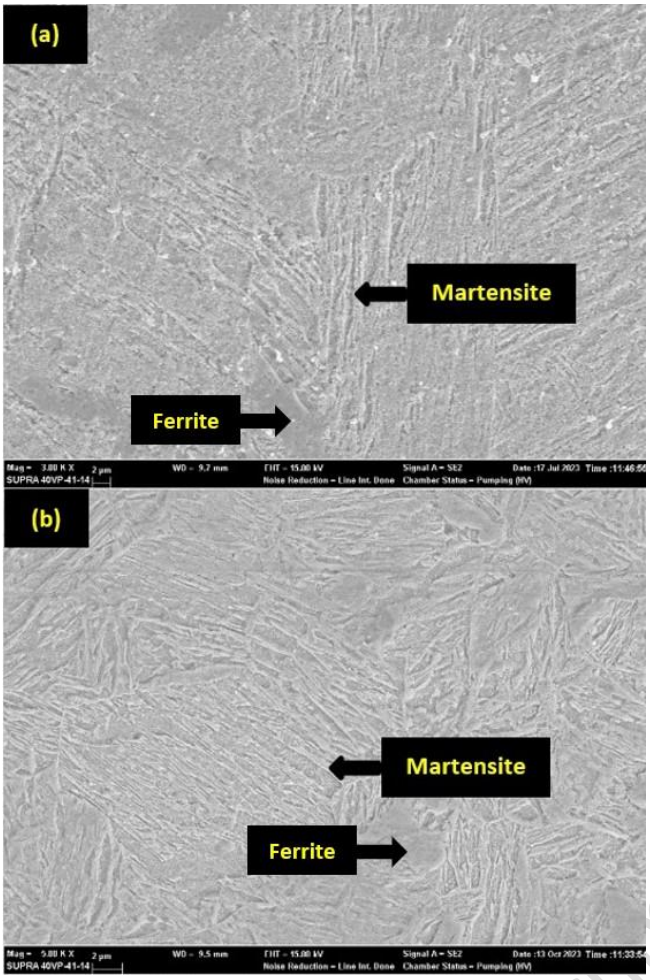

Figure 7. WM SEM images of RSW joints a) DP600/DP1000 b) DP600/DP1200.

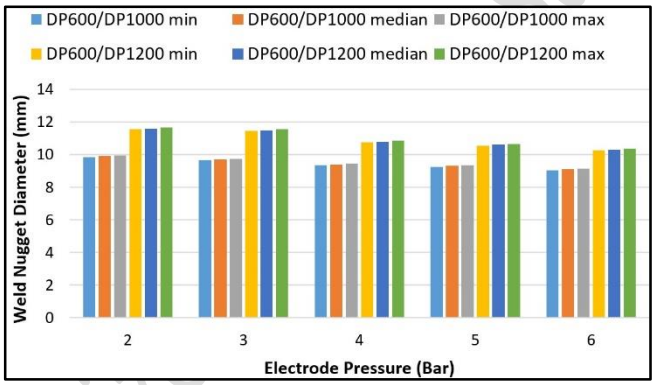

Figure 8. WN diameter values obtained at different EPs.

3.3 Tensile shear properties

Welds in the vehicle structures are subjected to both shear and tensile loading [5], [6], [28]. TST mainly refers to shear loading [29], [30]. WN diameter is a critical parameter affecting the TSS properties of RSW combinations [3], [27], [31]. As the WN diameter increases, the stress concentration factor around the notch root decreases, thus increasing the TSS [5], [24]. Looking at Figure 9, as the EP increases, the electrical resistance decreases, so the heat input decreases, and cannot melt the contact surface completely, instead the WN size decreases. As a result, the TSF values decreased for both types of joint. These results can also be interpreted in two ways. Firstly, a slightly inhomogeneous distribution of EP appeared around the spot weld during RSW [32]. Secondly, the loading capacity was reduced by oversized indentation[33]. The WN diameter and TSF values showed a linear relationship.

In addition, Ma et al. [2] found that the welds made with the lower EP had a greater number of micro-voids than those made with the higher EP. In the case of a lower EP, the WN may not be compressed enough to solidify before the electrodes are removed from the weld area, which can cause micro voids to form. Therefore, at values below 2 bar EP, micro-void formation can be observed which is detrimental to the TSF. However, at the EP values used in the current study, no micro-void formation occurred.

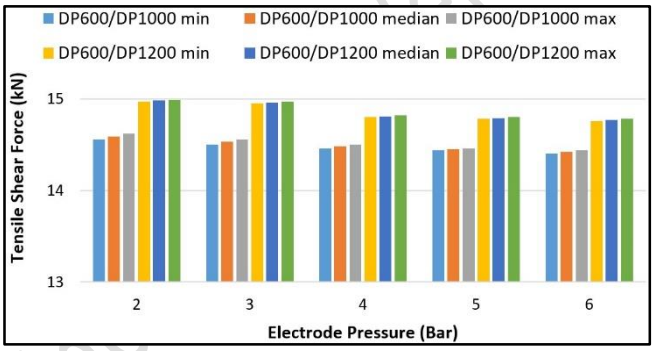

Figure 9. TSF values obtained at different EPs.

Due to the very high heat input, expulsion occurs in the RSW. Expulsion is a condition that negatively affects the quality of the joint [22], [34]. At low EP, the contact resistance was so high that the metal on the contact surface melted considerably due to the high input, while the plastic ring was too weak to contain the molten metal. So, at low EP, expulsion occurred. At high EP, the molten zone was crushed, and the plastic ring was unable to restrict the occurrence of expulsion[12]. Although the highest TSF values were obtained at 7kA WC-2 bar EP for both types of joint, expulsion did occur (Figure 10). Khan et al. [20] observed expulsion at around 7-9 kA WC values.

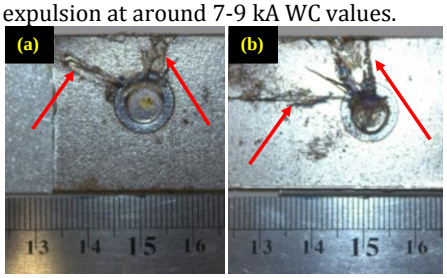

Figure 10. Expulsion images obtained at 2 bar EP for different joint types a) DP600/DP1000, b) DP600/DP1200.

3.4 Failure analysis

As a result of TST, IF and PF occur. To ensure RSW reliability in the industry, IF should be avoided. PF can be achieved by adjusting the process parameters. PF is desired for optimum structural performance [6]. This is because IF has a lower load carrying capacity than the PF [35].

As a result of the TST of the DP600/DP1000 and DP600/DP1200 RSW joints obtained at different EPs, the PF, which is preferred in terms of optimum structural performance, was observed in all specimens (Figure 11). Yuan et al. [12] and Zhang et al. [19] observed two different failure modes during TST of the joints: IF and PF. However, Li et al. [21]

observed only the IF mode during the TST of the joints. In all the joints, the failures occurred on the DP600 side, which has the lower strength value. Photographs of the failure surfaces are shown in Figure 11. However, Zhang et al. [19] found that for the DP780/DP600 RSW joints of similar thickness, the failure was initiated from the DP780 side.

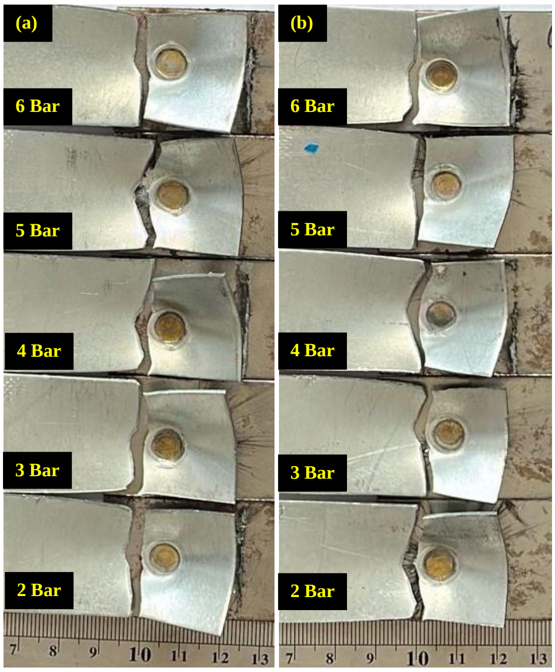

Figure 11. PF images obtained by TST a) DP600-DP1000, b) DP600-DP1200.

Knowledge of the failure mechanism is necessary to evaluate RSW joints. The failure mode affects the shape of the tail in tensile curves. In PF mode, the maximum point relates to the constriction of the nugget circumference[6], [36]. As a result of SEM analysis of the failure surfaces, dimples were observed indicating ductile failure (Figure 12b, Figure 13b). As PF occurred in all specimens, the failure surfaces of DP600/DP1000 and DP600/DP1200 joints obtained at 3 bar pressure were examined. SEM images showing crack initiation and dimples for the DP600/DP1000 and DP600/DP1200 combinations are shown in Figure 12 and Figure 13, respectively. Judging from Figure 12 and Figure 13, the driving force of PF is the tensile stress at the WM environment. Extensive plastic deformation and obvious necking occurred at the HAZ/BM interface because the HAZ/BM interface is weak at the joint. The grain orientation of the HAZ was obviously changed in contrast to that of the BM, and abnormally grown grains were found at the HAZ/BM interface. The abnormally grown grains led to the deterioration of mechanical properties, so that PF occurred along the weak HAZ/BM interface[12], [19].

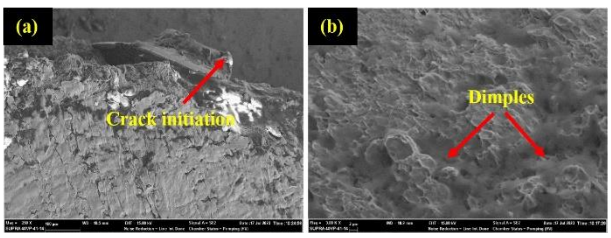

Figure 12. SEM images of DP600/DP1000 failure surfaces a) Crack initiation, b) Dimples.

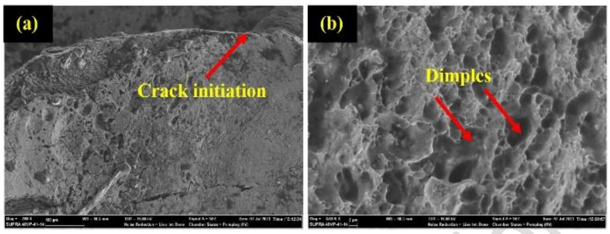

Figure 13. SEM images of DP600/DP1200 failure surfaces a) Crack initiation, b) Dimples.

3.5 Microhardness

The microhardness results obtained at different welding parameters are shown in Figure 14. The microhardness results were in agreement with the TSF values. The highest microhardness values were obtained at 7kA WC-2 bar EP for both types of joints. As can be seen, the hardness of WM increased after RSW. The hardness values increase from BM to WM due to the high heat input in the RSW process [6]. Martensitic transformation is a hardening and strengthening mechanism in steel. Strong and hard martensite is a good resistance barrier against movement and dislocation slip in the DP structure. During the RSW process, the very rapid heating and cooling cycle precipitates austenite into martensite transformation. In RSW, the WM cools from the austenite phase; the HAZ also cools due to the austenite and therefore these regions have higher hardness than the BM [22]. Similarly, Khan et al. [20] and Li et al. [21] reported that the higher hardness in the WM was due to martensite formation. Thus, the hardness values in all parameters increased from BM to WM. Zhang et al. [19] and Li et al. [21]reported that the hardness in the WM was significantly higher than that of the BM.

Yuan et al. [12] and Zhang et al. [19] found the average hardness values of WM on the DP600 side to be 315 HV and 361 HV respectively. However, in this study, the hardness values of WM on the DP600 side were found to be between 350-410 HV. Similarly, Li et al. [21] found the hardness values of WM on the DP600 side to be between 350-400 HV.

(a)

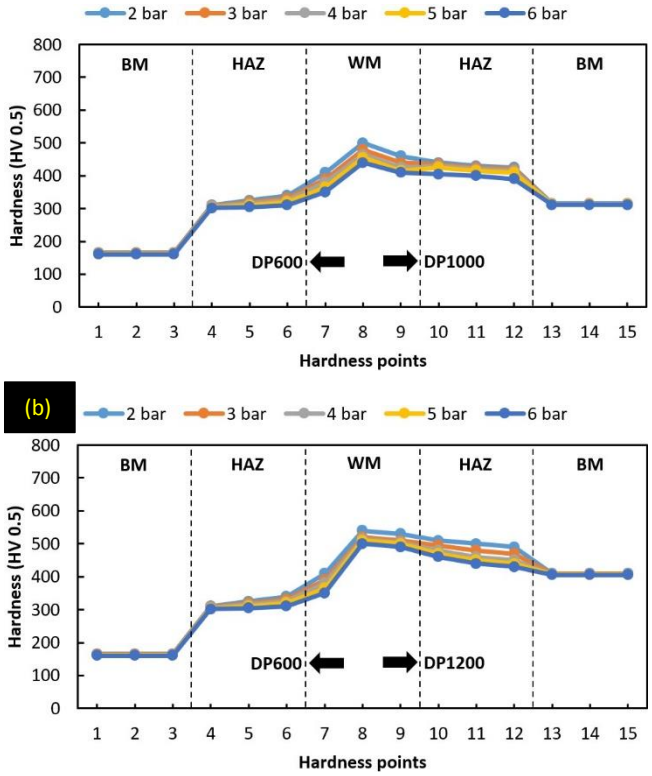

Figure 14. Microhardness values obtained at different EPs a) DP600/DP1000, b) DP600/DP1200.

4 Conclusions

The conclusions can be expressed as follows:

1. After the RSW process, three different microstructural regions, namely BM, HAZ, and WM, were observed in the welded joints.
2. It was observed that the BM microstructure of DP steels consisted predominantly of ferrite phase and a small amount of martensite phase. From BM to WM, the ferrite phase decreased, and the martensite phase increased due to the high temperature and subsequent rapid cooling.
3. EP was an important factor in controlling WN formation. As EP increased, the heat input at the sheet/sheet contact surface decreased. As a result, the WN diameter values decreased.
4. As the WN diameter increased, the TSF value increased. Therefore, the WN diameter values, and the TSF values showed a linear relationship. As EP increased, TSF decreased.
5. Although the highest TSF values were obtained at 2 bar EP for both types of joint, expulsion occurred due to excessive heat input. The expulsion negatively affected the quality of the weld.
6. The PF, which is preferred for optimum structural performance, was observed and failures occurred on the DP600 side, which has the lower strength value in all joints. Dimples indicating ductile failure were also observed.
7. Hardness values increased with increasing amount of martensite in the WM compared to the BM.

5 Author contribution statements

For this study, Author 1 contributed to the literature review, and the conduct of the experiments and Author 2 contributed to the generation of the idea, its design, the evaluation of the results obtained, and the analysis of the results.

6 Ethics committee approval and conflict of interest statement

"There is no need for ethics committee approval for the prepared article".

"There is no conflict of interest with any person/institution in the prepared article".

7 References

[1] Katılmış E. Investigation of Microstructure and Mechanical Properties of Dual Phase Steels with Different Strength Levels Joined by Resistance Spot Welding. MSc Thesis, Karabuk University, Karabuk, Türkiye, 2023.

[2] Ma C, Chen DL, Bhole SD, Boudreau G, Lee A, Biro E. "Microstructure and fracture characteristics of spot-welded DP600 steel". Materials Science and Engineering: A, 485(1–2), 334–346, 2008.

[3] Long X, Khanna SK. "Fatigue properties and failure characterization of spot-welded high strength steel sheet". International Journal of Fatigue, 29(5), 879–886, 2007.

[4] Demir B. An Investigation of Producibility of Dual-Phase Steel at the Continuous Annealing Line of Ereğli Iron and Steel Plant. PhD Thesis, Gazi University, Ankara, Türkiye, 2003.

[5] Demir B, Elitas M, Karakuş H. "Investigation of the tensile shear property of DP600 steel combined with resistance spot welding". Pamukkale University Journal of Engineering Sciences, 28(4), 533–538, 2022.

[6] Elitas M. "Effects of welding parameters on tensile properties and failure modes of resistance spot welded DC01 steel". Proceedings of the Institution of Mechanical Engineers, Part E: Journal of Process Mechanical Engineering, 237(4), 1607-1616, 2023.

[7] Boriwal L, Sarviya RM, Mahapatra MM. "Process analysis and regression modelling of resistance spot welded joints of austenitic stainless steel 304L and low carbon steel sheets by using surface response methodology". Proceedings of the Institution of Mechanical Engineers, Part E: Journal of Process Mechanical Engineering, 235(1), 24–33, 2021.

[8] Eisazadeh H, Hamedi M, Halvaee A. "New parametric study of nugget size in resistance spot welding process using finite element method". Materials & Design, 31(1), 149–157, 2010.

[9] Moshayedi H, Sattari-Far I. "Numerical and experimental study of nugget size growth in resistance spot welding of austenitic stainless steels". Journal of Materials Processing Technology, 212(2), 347–354, 2012.

[10] Krishnan V, Ayyasamy E, Paramasivam V. "Influence of resistance spot welding process parameters on dissimilar austenitic and duplex stainless steel welded joints". Proceedings of the Institution of Mechanical Engineers, Part E: Journal of Process Mechanical Engineering, 235(1), 12–23, 2021.

[11] Raoelison RN, Fuentes A, Pouvreau C, Rogeon P, Carre P, Dechalotte F. "Modeling and numerical simulation of the resistance spot welding of zinc coated steel sheets using rounded tip electrode: Analysis of required conditions". Applied Mathematical Modelling, 38(9-10), 2505–2521, 2014.

[12] Yuan X, Li C, Chen J, Li X, Liang X, Pan X. "Resistance spot welding of dissimilar DP600 and DC54D steels". Journal of Materials Processing Technology, 239, 31–41, 2017.
[13] Dancette S, Fabrègue D, Massardier V, Merlin J, Dupuy T, Bouzekri M. "Experimental and modeling investigation of the failure resistance of advanced high strength steels spot welds". Engineering Fracture Mechanics, 78(10), 2259–2272, 2011.
[14] Boriwal L, Sarviya RM, Mahapatra MM. "Weld bonding process analysis for tensile shear strength and peel strength of weld bonded joints of dissimilar steel sheets". Proceedings of the Institution of Mechanical Engineers, Part E: Journal of Process Mechanical Engineering, 233(4), 709–717, 2019.
[15] Zhou M, Zhang H, Hu SJ. "Relationships between quality and attributes of spot welds". Welding Journal, 82(4), 72-77, 2003.
[16] Sun X, Dong P. "Analysis of aluminum resistance spot welding processes using coupled finite element procedures". Welding Journal, 79(8), 215-221, 2000.
[17] Aydin H. "The mechanical properties of dissimilar resistance spot-welded DP600–DP1000 steel joints for automotive applications". Proceedings of the Institution of Mechanical Engineers, Part D: Journal of Automobile Engineering, 229(5), 599–610, 2015.
[18] Aydin K, Hidiroglu M, Kahraman N. "Characterization of the welding zone of automotive sheets of different thickness (DP600 and DP800) joined by resistance spot welding". Transactions of the Indian Institute of Metals, 75(5), 1279–1291, 2022.
[19] Zhang H, Wei A, Qiu X, Chen J. "Microstructure and mechanical properties of resistance spot welded dissimilar thickness DP780/DP600 dual-phase steel joints". Materials & Design (1980-2015), 54, 443–449, 2014.
[20] Khan MS, Bhole SD, Chen DL, Biro E, Boudreau G, Van Deventer J. "Welding behaviour, microstructure and mechanical properties of dissimilar resistance spot welds between galvannealed HSLA350 and DP600 steels". Science and Technology of Welding and Joining, 14(7), 616–625, 2009.
[21] Li T, Yuan X, Hu Z, Wu K, Wang H, Zhang B. "Dissimilar Resistance Spot Welding of DP 600/A5052/DP 600 Triple Sheets". International Journal of Precision Engineering and Manufacturing, 19(11), 1673–1679, 2018.
[22] Elitas M. "Effects of welding parameters on tensile properties and fracture modes of resistance spot welded DP1200 steel". Materials Testing, 63(2), 124–130, 2021.
[23] Elitas M, Demir B. "The effects of the welding parameters on tensile properties of RSW junctions of DP1000 sheet steel". Engineering, Technology & Applied Science Research, 8(4), 3116–3120, 2018.
[24] Elitas M, Erden MA. "Investigation of the effect of different welding parameters on tensile properties and failure modes of non-alloyed steel produced by powder metallurgy". Proceedings of the Institution of Mechanical Engineers, Part E: Journal of Process Mechanical Engineering, 237(5), 2074–2082, 2023.
[25] Dancette S, Fabrègue D, Massardier V, Merlin J, Dupuy T, Bouzekri M. "Investigation of the tensile shear fracture of advanced high strength steel spot welds". Engineering Failure Analysis, 25, 112–122, 2012.
[26] Pouranvari M, Marashi SPH. "Factors affecting mechanical properties of resistance spot welds". Materials Science and Technology, 26(9), 1137–1144, 2010.
[27] Pouranvari M, Marashi SPH. "Critical review of automotive steels spot welding: process, structure and properties". Science and Technology of Welding and Joining, 18(5), 361–403, 2013.
[28] Pouranvari M, Marashi SPH. "Failure of resistance spot welds: tensile shear versus coach peel loading conditions". Ironmaking & Steelmaking, 39(2), 104–111, 2012.
[29] Pouranvari M, Marashi SPH. "Failure mode transition in AISI 304 resistance spot welds". Welding Journal, 91(11), 303–309, 2012.
[30] Pouranvari M, Marashi SPH. "Failure mode transition in AHSS resistance spot welds. Part I. Controlling factors". Materials Science and Engineering: A, 528(29–30), 8337–8343, 2011.
[31] Hilditch TB, Speer Jy, Matlock DK. "Effect of susceptibility to interfacial fracture on fatigue properties of spot-welded high strength sheet steel". Materials & Design, 28(10), 2566–2576, 2007.
[32] Huin T, Dancette S, Fabrègue D, Dupuy T. "Investigation of the failure of advanced high strength steels heterogeneous spot welds". Metals, 6(5), 111, 2016.
[33] Zhao DW, Wang YX, Zhang L, Zhang P. "Effects of electrode force on microstructure and mechanical behavior of the resistance spot welded DP600 joint". Materials & Design, 50, 72–77, 2013.
[34] Zhao D, Wang Y, Liang D, Zhang P. "An investigation into weld defects of spot-welded dual-phase steel". The International Journal of Advanced Manufacturing Technology, 92(5–8), 3043–3050, 2017.
[35] Pouranvari M, Marashi SPH. "Minimum fusion zone size required to ensure pullout failure mode of resistance spot welds during tensile-shear test". Kovove Materialy-Metallic Materials, 48, 197–202, 2010.
[36] Pouranvari M, Marashi SPH, Mousavizadeh SM. "Dissimilar resistance spot welding of DP600 dual phase and AISI 1008 low carbon steels: correlation between weld microstructure and mechanical properties". Ironmaking & Steelmaking, 38(6), 471–480, 2011.